SAND2017-9632C

Power System Damping Control via Current Injections from Distributed Energy Storage

David A. Copp, Felipe Wilches-Bernal, and David A. Schoenwald

***Abstract*—Inter-area oscillations are present in all power systems dispersed over large areas and can have detrimental effects limiting transmission capacity or even causing blackouts. The availability of wide-area measurements in power systems has enabled damping of inter-area oscillations using distributed control methods and system components, such as energy storage devices. We investigate the performance of damping control enabled by energy storage devices distributed throughout an example two-area power system assuming the availability of wide-area measurements of generator machine speeds. The energy storage devices are capable of injecting current into the system in order to damp inter-area oscillations that occur after a fault in the system. Several simulations of the nonlinear system with multiple combinations of energy storage providing current injections are performed. From the numerical results, we quantify and discuss how damping performance depends on the location, size, and number of injections.**

I. Introduction

Power systems consist of complex interconnections of nonlinear components, possibly sparsely distributed across wide geographic regions. This means that power loads and generation may be geographically separated by large distances. In these systems, an event, such as a fault at one of the buses, results in swings in the power transfer between regions. These power swings are called inter-area oscillations [1], and they occur in power systems around the world. Damping inter-area oscillations is crucial for maintaining a secure and reliable power grid, and failing to do so can have severe consequences, such as the blackouts experienced throughout western North America in 1996 [2].

Several methods for implementing damping control that mitigate the effects of inter-area oscillations have been proposed. Power System Stabilizers (PSSs), utilizing local measurements, have historically been used to implement damping control. More recently, the use of remote signals with PSSs has been shown to be advantageous [3]. The availability of system-wide information via remote signals has enabled the use of other system components for damping control, such as Flexible AC Transmission Systems (FACTS) devices, High Voltage DC (HVDC) lines, and Energy Storage (ES) [4]–[10].

In this work, we specifically investigate damping control enabled by current injections from ES devices distributed throughout the system. The damping control law is based on feedback from wide-area measurements of the generators' machine speeds. Naturally, injections from ES devices in different locations throughout the system result in different transient responses and, thus, different damping performance. With multiple ES devices available throughout the system, there may be scenarios in which it is advantageous to use smaller current injections from more ES devices distributed throughout the system rather than using larger current injections from fewer ES devices. We quantify performance for these types of scenarios and provide insights for how best to utilize ES devices for damping control in this example system. Specifically, we perform nonlinear simulations of the two-area example power system with damping control enabled by current injections from multiple ES devices; we quantify the damping performance of several combinations of ES devices providing current injections, discuss how performance depends on the number, sizes, and locations of injections, and show that there are diminishing improvements on damping performance as the size of current injections increase.

Several authors have previously investigated the use of ES devices for damping control of power systems similar to the one considered in this work. Damping with an ES device using particle swarm optimization and heuristic dynamic programming is discussed to be better than PSS or FACTS enabled damping in [11] for the same example system and signals that we consider. An ES system based on UltraCapacitor technology is utilized for damping control via real power modulation in [10]. The same authors show that the optimal placement for an ES device to provide damping in a power system is in the area with lower inertia [12]. The authors of [13] consider a similar system with only one ES device in each area and show that the inter-area oscillations can be effectively damped and that the best locations for the ES devices along the tie line are closer to the generators. In this work we extend these previous results by investigating injections from multiple ES devices distributed throughout the system. Several other power and energy applications of ES as well as optimal energy management with ES are discussed in [14], and multiple applications and value opportunities for ES are highlighted in [15].

This paper is organized as follows. First we formulate the problem by introducing the example two-area power system and damping control law under consideration in Section II. Next we present numerical results and quantify damping control performance in Section III. Finally, Section IV contains concluding remarks and directions for future work.

D. Copp, F. Wilches-Bernal, and D. Schoenwald are with Sandia National Laboratories, Albuquerque, NM (e-mail: dcopp@sandia.gov). Sandia National Laboratories is a multi-mission laboratory managed and operated by National Technology and Engineering Solutions of Sandia, LLC., a wholly owned subsidiary of Honeywell International, Inc., for the U.S. Department of Energy's National Nuclear Security Administration under contract DE-NA-0003525.

II. Problem Formulation

A. Two-Area Power System Model

We analyze the power system shown in Figure 1, which contains two areas, with two synchronous generators and a load in each area, as well as six ES devices distributed throughout the system. The synchronous generators are located at buses 1, 2, 3, and 4, respectively. The loads are located at buses 18 and 19, respectively, and the ES devices are located at buses 12, 13, 14, 15, 16, and 17, respectively. The ES devices are capable of injecting current into the system in order to damp inter-area oscillations. We excite the system by applying a ground bus fault at bus 7, which causes inter-area oscillations, and investigate the damping performance when different combinations of ES devices provide current injections. For example, we quantify the differences in control effort (current injected) and transient system response when all six of the ES devices provide current injections versus when only ES devices 1 and 6 provide current injections.

Each synchronous generator i is modeled using a subtransient model, and the dynamics are given by

$$\begin{aligned} \dot{x}_i(t) &= f(x_i(t), u(t)), \\ y_i(t) &= \omega_i(t), \end{aligned} \tag{1}$$

where $x_i(t) = [\delta_i(t)\ \omega_i(t)\ E'_{q,i}(t)\ \psi''_{d,i}(t)\ E'_{d,i}(t)\ \psi''_{q,i}(t)]^\top$ denotes the state vector of the i^{th} generator at time t with the states being the generator angle δ_i, generator angular velocity ω_i, quadrature axis transient terminal voltage $E'_{q,i}$, direct axis subtransient flux linkage $\psi''_{d,i}$, direct axis transient terminal voltage $E'_{d,i}$, and quadrature axis subtransient flux linkage $\psi''_{q,i}$. The vector of current injections at time t is denoted by $u(t) = [u_1(t)\ u_2(t)\ u_3(t)\ u_4(t)\ u_5(t)\ u_6(t)]^\top$, and the output at time t is denoted by $y_i(t)$. The output for generator i is its angular velocity, so the (possibly remote) measurements of the generators' angular velocities are available for feedback. For brevity we do not explicitly write down the nonlinear function $f(\cdot)$ in (1), but more details on these dynamics can be found in, e.g., [1], [16].

The model parameters are chosen to be the same as in Example 12.6 of [1] and are given in Table I. Except for the inertia constants H_1, H_2, H_3, and H_4, all of the parameter values are the same for all four of the generators. Saturation effects are neglected.

B. Damping Control Law

The damping control law for the current injection from the i^{th} ES device is given by

$$u_i(t) = \begin{cases} \frac{k_d}{\mathcal{I}_1}(\Omega_1(t) - \Omega_2(t)), & \text{if injection in area 1,} \\ \frac{k_d}{\mathcal{I}_2}(\Omega_2(t) - \Omega_1(t)), & \text{if injection in area 2,} \end{cases}$$

where $\Omega_1(t)$ and $\Omega_2(t)$ are the average angular velocities of the generators in areas 1 and 2 at time t (i.e., $\Omega_1(t) = \frac{\omega_1(t)+\omega_2(t)}{2}$ and $\Omega_2(t) = \frac{\omega_3(t)+\omega_4(t)}{2}$), respectively, $\mathcal{I}_1$ and $\mathcal{I}_2$ are the number of injections in areas 1 and 2, respectively, and k_d is the damping control gain. Therefore, the magnitude of each current injection is scaled by the number of injections in the area in which it is located; i.e., if there are three injections in area 1, the value of $k_d/\mathcal{I}_1 = k_d/3$, whereas if there is only one injection in area 1, $k_d/\mathcal{I}_1 = k_d$. In this way, the sum of the current injections, calculated based on the difference between Ω_1 and Ω_2, will be the same in each area regardless of the number of injections in that area. This is done so as to address the question of how performance changes when injecting all of the current in one location versus injecting the same total amount of current but through several injections distributed throughout the system.

Figure 2 shows a block diagram of the current injections from the ES devices. In Figure 2, Ω_i denotes the average of the angular velocities of the generators in area i, Ω_j denotes the average of the angular velocities of the generators in the other area, and T denotes the response time of the ES devices. The transfer function $1/(1 + Ts)$, where s is the Laplace transform variable, acts as a first-order low-pass filter that captures the dynamics of the injection. In this work, we choose $T = 0.05$ [s], which is representative of the response time of, e.g., Superconducting Magnetic Energy Storage (SMES) [9]. The signal $\bar{u}_i(t)$ then denotes the current injection of ES device i into the system.

TABLE I
Model Parameters

Generators:			
Parameter	Description	Value	Units
P_r	power rating	900	MVA
X_d	direct axis synchronous reactance	1.8	per unit
X_q	quadrature axis synchronous reactance	1.7	per unit
X_l	leakage reactance	0.2	per unit
X'_d	transient reactance	0.3	per unit
X'_q	transient reactance	0.55	per unit
X''_d	subtransient reactance	0.25	per unit
X''_q	subtransient reactance	0.25	per unit
R_a	armature resistance	0.0025	per unit
T'_{d0}	open-circuit time constant	8.0	seconds
T'_{q0}	open-circuit time constant	0.4	seconds
T''_{d0}	open-circuit subtransient time constant	0.03	seconds
T''_{q0}	open-circuit subtransient time constant	0.05	seconds
H_1, H_2	inertia constant	6.5	per unit
H_3, H_4	inertia constant	6.175	per unit
K_D	damping coefficient	0	per unit
Transmission:			
Parameter	Description	Value	Units
r	line resistance	0.0001	per unit/km
x_L	line reactance	0.001	per unit/km
b_C	line charging	0.00175	per unit/km
z_T	transformer impedance	0.0167	per unit/km
System:			
Parameter	Description	Value	Units
S_b	system base MVA	100	MVA
S_f	system frequency	60	Hz

III. Numerical Results

In this section we present numerical results from simulating the example two-area power system shown in Figure 1. We

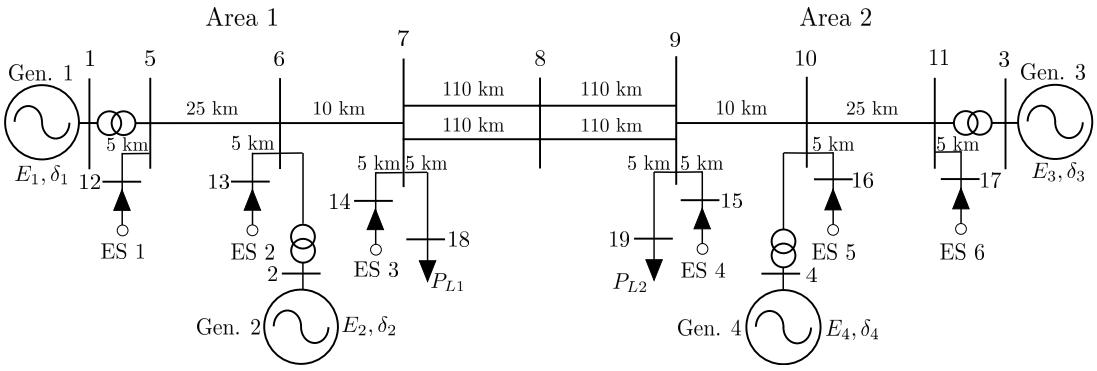

Fig. 1. Example two-area power system.

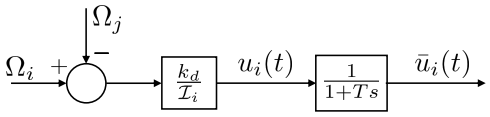

Fig. 2. Block diagram of current injections from ES devices.

analyze a 15 second window in which the system is excited by a ground bus fault at bus 7 at $t = 0.5$ [s] with clearing times of 0.005 [s] at the near end of the system and 0.01 [s] at the remote end of the system. After the fault, we investigate the effect that current injections from multiple combinations of ES devices have on the system's damping. We acknowledge that there are 720 different ES injection combinations available, but we only present 25 different combinations that are representative of the options available. All simulations of the nonlinear system are performed using the Power System Toolbox [17] in MATLAB.

The initial conditions of the system are as follows: The initial load in area 1 is $(P_{L1}, Q_{L1}) = (12.67, 1.00)$ [pu], the initial load in area 2 is $(P_{L2}, Q_{L2}) = (14.67, 1.00)$ [pu], and the generators are loaded as follows (all values are in per unit):

$$\begin{aligned} P_1 &= 7 \quad Q_1 = 1.85 \quad V_1 = 1.03\angle 20.2^\circ \\ P_2 &= 7 \quad Q_2 = 2.35 \quad V_2 = 1.01\angle 10.5^\circ \\ P_3 &= 7 \quad Q_3 = 1.76 \quad V_3 = 1.03\angle -6.8^\circ \\ P_4 &= 7 \quad Q_4 = 2.02 \quad V_4 = 1.01\angle -17^\circ \end{aligned}$$

Results are shown for two values of the control gain: $k_d = 200$ and $k_d = 500$. The value $k_d = 200$ is chosen because it results in the maximum current injection being about 0.05 [pu]. This is appropriate as a user may not want to allocate more than 5% of the ES device's rated power for damping control. The value $k_d = 500$ is chosen to show how much damping performance improves when larger injections are considered.

Table II shows damping control performance results from a numerical analysis of the two-area power system shown in Figure 1 after a ground bus fault occurs at bus 7 with damping control via current injections from ES devices, as shown in Figure 2. The rows are organized by resulting performance

TABLE II
PERFORMANCE RESULTS (ALL VALUES ARE IN PER UNIT)

	$k_d = 200$		$k_d = 500$	
ES injections	$\|\Omega_1 - \Omega_2\|_2$	$\|u\|_{\max}$	$\|\Omega_1 - \Omega_2\|_2$	$\|u\|_{\max}$
1,6	0.00298	0.055	0.00239	0.135
1,2,5,6	0.00310	0.028	0.00249	0.068
1,3,4,6	0.00321	0.028	0.00260	0.068
1,2,3,4,5,6	0.00322	0.018	0.00260	0.045
2,5	0.00324	0.055	0.00261	0.136
3,4,6	0.00336	0.055	0.00274	0.136
1,3,4	0.00337	0.055	0.00274	0.136
3,4,5,6	0.00337	0.055	0.00274	0.136
1,2,3,4	0.00337	0.055	0.00274	0.136
2,3,4,5	0.00338	0.028	0.00275	0.068
6	0.00343	0.056	0.00281	0.137
3,4,5	0.00347	0.056	0.00283	0.137
2,3,4	0.00347	0.056	0.00283	0.137
1	0.00349	0.056	0.00287	0.137
5,6	0.00354	0.028	0.00291	0.069
3,4	0.00357	0.056	0.00293	0.137
1,2	0.00362	0.028	0.00298	0.069
4,6	0.00366	0.028	0.00302	0.069
4,5,6	0.00367	0.019	0.00302	0.046
5	0.00369	0.056	0.00304	0.137
1,3	0.00374	0.028	0.00310	0.069
1,2,3	0.00375	0.019	0.00311	0.046
2	0.00377	0.056	0.00313	0.138
4,5	0.00383	0.028	0.00317	0.069
2,3	0.00393	0.028	0.00328	0.069
none	0.00549	0	0.00549	0

so that the combination of ES devices that produce the best results are at the top, and the result with no injections is at the bottom. The first column shows the combination of ES injections used. The second and fourth columns show the value of the 2-norm of the difference between Ω_1 and Ω_2, thereby quantifying damping performance. Finally, the third and fifth columns show the value of the max-norm of the input vector u for the entire simulation (i.e., the maximum absolute value of u), thereby quantifying the size of the largest injection commanded by the damping controller.

Figure 3 shows responses of the system after the fault for the cases when no ES devices inject current and when three different combinations of ES devices inject current. Figure 4 shows the corresponding injections that produce two of the responses shown in Figure 3. Results with $k_d = 200$ are

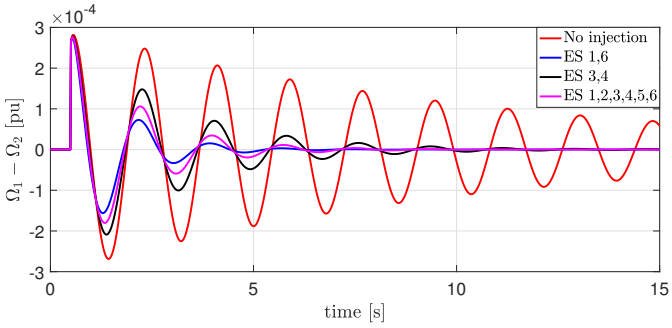

(a) $k_d = 200$

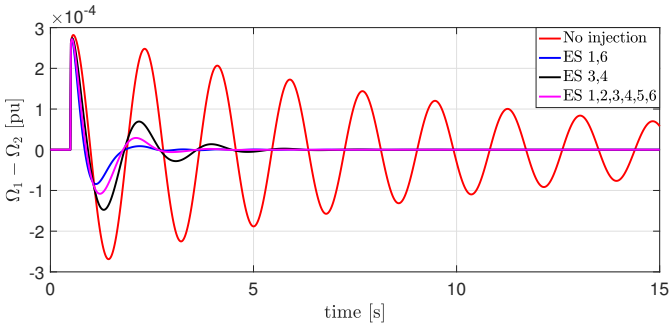

(b) $k_d = 500$

Fig. 3. Difference between the average machine speed in area 1 and area 2 after the fault. Injections from only ES devices 1 and 6 provide the best damping, while injections from all six ES devices provide better damping than injections from only ES devices 3 and 4.

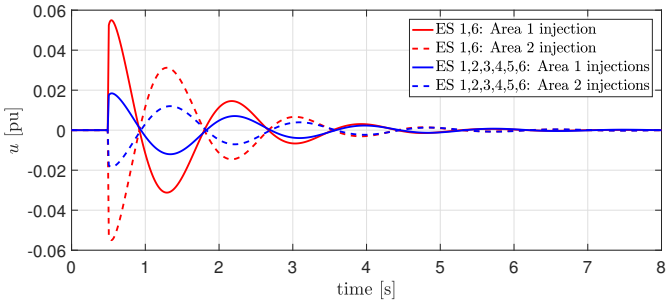

(a) $k_d = 200$

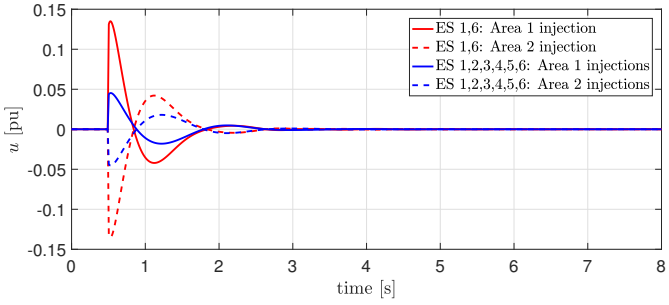

(b) $k_d = 500$

Fig. 4. Current injections when ES devices 1 and 6 are used (red) and when all six ES devices are used (blue). Note that the scales on the y-axes are different.

shown in Figures 3(a) and 4(a), and results with $k_d = 500$ are shown in Figures 3(b) and 4(b). Naturally, increasing the control gain k_d increases the size of the injections, and the damping performance improves.

A. Discussion

The first main takeaway from these results is that any injections from ES devices improve the damping performance regardless of how many or where they are located. In order to get the best improvement in damping performance, however, the number of injections and their locations are crucial as, depending on the choice of these options, damping performance may improve 28.4% to 45.7% when $k_d = 200$ and 40.3% to 56.5% when $k_d = 500$. This also shows that carefully choosing the number and locations of smaller injections can produce better damping performance than larger injections that are not carefully chosen. For example, injections from ES 1 and 6 with $k_d = 200$ produce better results than injections from ES 4 and 6 with $k_d = 500$, and the largest injections are 1.25 times smaller.

All of these results are consistent with the results in [12]; better performance is achieved when using injections from ES devices in the area with lower inertia. This is easy to see in our example because the network is symmetric. In this example, area 2 has lower inertia, so using only an injection from ES 6 produces better results than using only an injection from ES 1. Similarly, using only an injection from ES 5 produces better results than using only an injection from ES 2. The same is true for multiple injections in each area; injections from ES 5 and ES 6 provide better results than injections from ES 1 and ES 2, etc. Figure 5 shows some of these results when $k_d = 200$ and $k_d = 500$.

As we saw previously, there is a natural correlation between the size of injections and the damping performance. In general, larger injections produce better damping performance; however, there are diminishing returns on damping performance as the size of injections increase. Figure 6 shows how the improvement in damping performance diminishes as the size of the largest injection increases. Furthermore, a number of smaller injections may perform damping almost as well as fewer larger injections, and, because the injections are smaller, may require smaller and less expensive ES devices. For instance, when $k_d = 200$, the best performance is achieved using injections from ES 1 and ES 6, and the damping is improved by 45.7% over the scenario where there are no injections. However, when considering injections from ES 1, ES 2, ES 5, and ES 6, the largest injections are half the size, and yet, the performance is still 43.5% better than having no injections. Assuming ES devices that are half the size of other ES devices are less than half the cost, savings can be realized. Additionally, using injections from all six ES devices produces 41.4% improved damping performance over the case of no injections, and the largest injections are three times smaller than when only injections from ES 1 and ES 6 are considered.

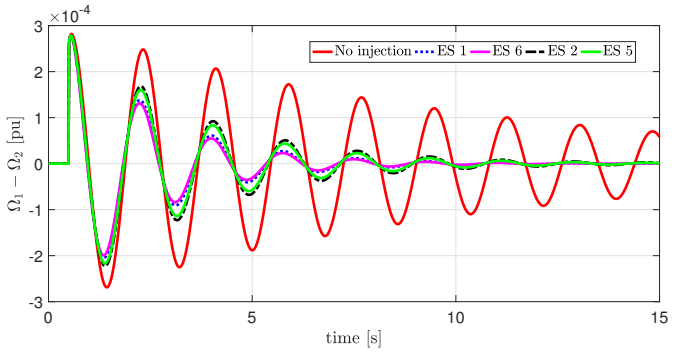

(a) $k_d = 200$

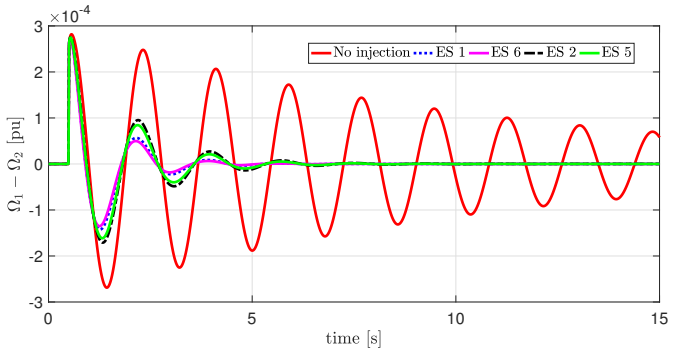

(b) $k_d = 500$

Fig. 5. Injections in the area with lower inertia (Area 2) result in better damping performance than injections in the area with higher inertia (Area 1).

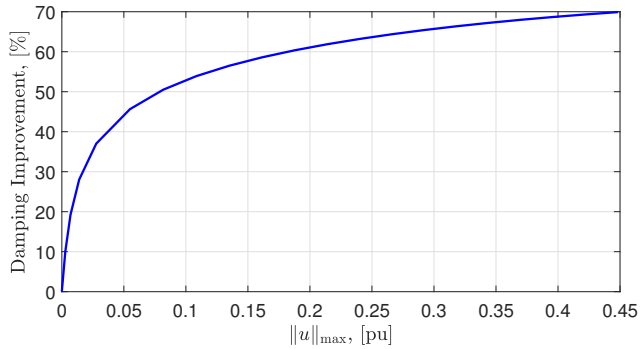

Fig. 6. Percentage improvement in damping performance for injections from ES 1 and ES 6, as compared to no injections, for different values of $\|u\|_{\max}$. These values of $\|u\|_{\max}$ result from choosing control gains from $k_d = 0$ to $k_d = 1700$.

IV. Conclusion

We investigated the use of current injections from distributed ES devices for damping inter-area oscillations in a representative two-area power system example assuming the availability of wide-area measurements of the generators' machine speeds. We looked at the effect that different numbers of injections as well as ES location and size have on the damping performance. We performed nonlinear simulations of the system subjected to a ground bus fault. Performance was quantified by computing the 2-norm of the difference between the average machine speeds in each of the two areas as well as the resulting maximum current injection size. Damping improves with any size or number of injections, but the damping performance depends greatly on the size, location, and number of injections. We discussed the trade-offs between choosing different numbers, sizes, and locations of injections.

For simplicity we did not consider constraints on the ES devices, such as maximum injection sizes, ramp rates, or power factors. In future work, optimization-based approaches will be considered that can explicitly address these constraints.

V. Acknowledgment

Funding for this research was provided by the US DOE Energy Storage Program managed by Dr. Imre Gyuk of the DOE Office of Electricity Delivery and Energy Reliability.

References

[1] P. Kundur, *Power System Stability and Control*. New York, NY: McGraw-Hill, 1994.

[2] D. N. Kosterev, C. W. Taylor, and W. Mittelstadt, "Model validation for the August 10, 1996 WSCC system outage," *IEEE Transactions on Power Systems*, vol. 14, no. 3, pp. 967–979, Aug. 1999.

[3] J. H. Chow, J. J. Sanchez-Gasca, H. Ren, and S. Wang, "Power system damping controller design using multiple input signals," *IEEE Control Systems Magazine*, vol. 20, no. 4, pp. 82–90, Aug. 2000.

[4] A. Chakrabortty, "Wide-area damping control of power systems using dynamic clustering and TCSC-based redesigns," *IEEE Trans. Smart Grid*, vol. 3, no. 3, pp. 1503–1514, Sept. 2012.

[5] D. Trudnowski, D. Kosterev, and J. Undrill, "PDCI damping control analysis for the western North American power system," in *Power and Energy Soc. General Meeting, IEEE*, Vancouver, BC, 2013, pp. 1–5.

[6] D. Trudnowski, B. Pierre, F. Wilches-Bernal, D. Schoenwald, R. Elliott, J. Neely, R. Byrne, and D. Kosterev, "Initial closed-loop testing results for the Pacific DC Intertie wide area damping controller," in *Power and Energy Soc. General Meeting, IEEE*, Chicago, IL, 2017, pp. 1–5.

[7] D. A. Schoenwald, B. J. Pierre, F. Wilches-Bernal, and D. J. Trudnowski, "Design and implementation of a wide-area damping controller using high voltage DC modulation and synchrophasor feedback," in *2017 IFAC World Congress*, 2017.

[8] A. M. Vural, "Contribution of high voltage direct current transmission systems to inter-area oscillation damping: A review," *Renewable and Sustainable Energy Reviews*, vol. 57, pp. 892–915, 2016.

[9] P. F. Ribeiro, B. K. Johnson, M. L. Crow, A. Arsoy, and Y. Liu, "Energy storage systems for advanced power applications," *Proceedings of the IEEE*, vol. 89, no. 12, pp. 1744–1756, 2001.

[10] J. Neely, R. Byrne, R. Elliott, C. Silva-Monroy, D. Schoenwald, D. Trudnowski, and M. Donnelly, "Damping of inter-area oscillations using energy storage," in *Power and Energy Soc. General Meeting, IEEE*, Vancouver, BC, 2013, pp. 1–5.

[11] X. Sui, Y. Tang, H. He, and J. Wen, "Energy-storage-based low-frequency oscillation damping control using particle swarm optimization and heuristic dynamic programming," *IEEE Transactions on Power Systems*, vol. 29, no. 5, pp. 2539–2548, September 2014.

[12] R. H. Byrne, D. Trudnowski, J. Neely, R. Elliott, D. Schoenwald, and M. Donnelly, "Optimal locations for energy storage damping systems in the Western North American interconnect," in *IEEE Power and Energy Soc. General Meeting*. IEEE, 2014, pp. 1–5.

[13] J. Wu, J. Wen, H. Sun, and S. Cheng, "Feasibility study of segmenting large power system interconnections with AC link using energy storage technology," *IEEE Transactions on Power Systems*, vol. 27, no. 3, pp. 1245–1252, 2012.

[14] R. H. Byrne, T. A. Nguyen, D. A. Copp, B. R. Chalamala, and I. Gyuk, "Energy management and optimization methods for grid energy storage systems," *IEEE Access*, in press, 2017.

[15] Electric Power Research Institute, "Electrical energy storage technology options," http://www.epri.com, Tech. Rep., December 2010.

[16] P. M. Anderson and A. A. Fouad, *Power system control and stability*. John Wiley & Sons, 2008.

[17] J. H. Chow and K. W. Cheung, "A toolbox for power system dynamics and control engineering education and research," *IEEE Transactions on Power Systems*, vol. 7, no. 4, pp. 1559–1564, Nov. 1992.